PHYSICAL REVIEW B VOLUME 21, NUMBER 8 15 APRIL 1980

Microscopic theory of thermal desorption and dissociation processes catalyzed by a solid surface

Gopa Sarkar De and Uzi Landman
School of Physics, Georgia Institute of Technology, Atlanta, Georgia 30332

Mark Rasolt
Solid State Division, Oak Ridge National Laboratory, Oak Ridge, Tennessee 37830

(Received 2 October 1979)

A microscopic model of thermal desorption and dissociation from metallic surfaces which exhibits explicit dependences on characteristic parameters of the adsorption system is developed. The evaluation of the rates of these processes involves: (i) a derivation of the thermal adatom-solid coupling, (ii) a stochastic incoherent multiphonon mechanism for the evolution of an excitation for bond rupture, and (iii) coupling to final-state reaction channels. Transition probabilities and rates obtained by using both truncated-harmonic and Morse-potential descriptions of the chemisorptive bond are presented and compared with experimental data for xenon and potassium desorption from a tungsten substrate. The results show agreement with experiment and exhibit a linear relationship of the logarithm of the rate versus inverse temperature.

I. INTRODUCTION

The fundamental understanding of the mechanisms of surface-catalyzed reactions is one of the major objectives of past and current surface-science studies. The three main methodologies which have been developed towards that goal can be classified as: (i) Phenomenological kinetic approach,[1,2] which consists of a reaction scheme and a corresponding system of kinetic equations which incorporate rate constants and species concentrations. In this class of studies the rate constants are regarded as parameters to be determined by fitting the solutions of the kinetic equations to experiments performed at a number of system conditions (temperature, pressure, etc.). (ii) Thermodynamical and statistical-mechanical approaches,[2-9] in which rate constants (at equilibrium) are evaluated using statistical quantities such as partition functions in juxtaposition with certain models of the reaction. Most notable among these methods are the transition-state theory[2] and "phase-space theories", Rice-Ramsperger-Kassel-Marcus (RRKM) and variants thereof,[10] and theoretical trajectory analysis[11] (although the latter, RRKM in particular, while most popular in gas-phase kinetics, have not been thoroughly investigated in surface-reaction studies). (iii) Microscopic models of the reaction mechanism.[12-22] In these theories the underlying physical processes governing the reacting system (such as, excitation, energy transfer, mode-mode couplings, transport) are investigated and an expression for the reaction rate is derived.

While all the above provide valuable information, it is obvious that the microscopic models carry the largest potential of providing fundamental understanding of the reaction processes. Studies of this kind would allow the investigation of the dependence of reaction paths and rates on characteristics of the reaction system and could provide *criteria* for matching catalytic partners and ambient conditions such as to allow for optimal catalytic selectivity and specificity. It should be recognized, however, that studies of type (iii) present great theoretical difficulties and thus are scarce. Nevertheless, current advents of theoretical methods and novel surface experimental techniques, in particular electronic and vibrational spectroscopies (ultraviolet photoemission, Auger chemical shifts, electron-loss spectroscopies, surface infrared techniques—to name a few)[23,24] and kinetic measurements (molecular beams[25] and mass- and state-selective spectroscopies), provide the impetus for an increased activity in the above direction.

In discussing the kinetics of a reaction it is convenient to formulate it in terms of elementary reaction steps.[1,25] For a surface reaction, typical elementary reaction steps are: adsorption, transport (diffusion), excitation, dissociation, association, and desorption, not all of which necessarily occur for one given reaction. In the present study we focus on bond-rupture elementary reactions, i.e., dissociation and desorption.[26] Moreover, we investigate the thermal phenomena as distinct from the corresponding induced processes[26(a)]: electron-stimulated desorption (ESD), electron-impact desorption (EID), photodesorption (PD), and field desorption (FD). In the present study we formulate a theory of thermal desorption processes, which exhibits explicitly the dependence on the rates on parameters characteristic to the adsorption system.

To facilitate our discussion we specify the following ingredients of the theory (a) coupling of an atom or a molecule to the surface, (b) substrate-induced thermal-energy transfer and excitation, and (c) temporal evolution of the system, i.e., time evolution and calculation of reactional probabilities and rates. Accordingly, the organization of the paper is as follows: The Hamiltonian and couplings are derived in Sec. II. Models of the excitation mechanism and temporal evolution yielding expressions for reaction rates are discussed in Sec. III. A systematic analysis and discussion of results of the models and further remarks are given in Sec. IV.

II. HAMILTONIAN AND COUPLINGS

A. Hamiltonian

The first step in our formulation is a statement of the Hamiltonian of the system. The total Hamiltonian of the adsorption system may be written as

$$H=T_e+T_N+V(\vec{r},\vec{R})\,, \tag{2.1}$$

where T_e and T_N represent kinetic energies of electrons and nuclei of the system (molecule and substrate) and $V(\vec{r},\vec{R})$, various contributions to the potential energy ($\vec{r}\equiv\{\vec{r}_M,\vec{r}_s\}$, $\vec{R}\equiv\{\vec{R}_M,\vec{R}_s\}$, where $\vec{r}_M$ and $\vec{r}_s$ are the electronic coordinates of the adsorbed molecule and solid respectively, and $\vec{R}_M$, $\vec{R}_s$ the corresponding nuclear coordinates). In the adiabatic approximation the total wave function is taken as[27]

$$\psi(\vec{r},\vec{R})=\phi(\vec{r},\vec{R})\chi_N(\vec{R})\,. \tag{2.2}$$

The electronic wave function satisfies the equation

$$[\,T_e+V(\vec{r},\vec{R})]\,\phi(\vec{r},\vec{R})=\epsilon_e(\vec{R})\phi(\vec{r},\vec{R}) \tag{2.3}$$

solved for fixed $\vec{R}$, where the direct interaction between nuclei is included in $V(\vec{r},\vec{R})$. The equation for the nuclear motion can be found variationally[28]

$$\left(-\sum_{\mu=1}^{N}\frac{1}{2M_\mu}\nabla_\mu^2+[\epsilon_e(\vec{R})+V'(\vec{r})]\right)\chi_N(\vec{R})=\epsilon_N\chi_N(\vec{R})\,, \tag{2.4}$$

where

$$V'(\vec{R})=\sum_{\mu=1}^{N}\int d\vec{r}\,\phi^*\left(-\frac{1}{2M_\mu}\nabla_\mu^2\right)\phi\,, \tag{2.5}$$

and the summations are over all the nuclei. The effective potential [expression in square brackets in Eq. (2.4)] for the nuclear motion is dominated by the electronic energy $\epsilon_e(\vec{R})$ and the term $V'(\vec{R})$ is small. It is interesting to note here that the *exact* eigenvalue ϵ_{exact} is bounded between ϵ_N [the solution to Eq. (2.4)] and ϵ'_N [the solution to Eq. (2.4) with $V'(R)$ neglected]; i.e., $\epsilon_N\geq\epsilon_{\text{exact}}\geq\epsilon'_N$.[29]

At this stage the electronic energy $\epsilon_e(\vec{R})$ may be modeled in the following manner. First one identifies in $\epsilon_e(\vec{R})$ those components which correspond to intramolecular bonds and to binding between atoms of the molecule and a localized region in the solid. The electronic interactions for a fixed configuration of nuclear molecular coordinates $\{\vec{R}_M\}$ and solid nuclear coordinates $\{\vec{R}_s\}$ determine the adsorption potential between the solid and the adsorbate. We separate the interaction into two parts: one in which the solid is kept stationary and the other where the solid is allowed to vibrate. It is via the latter contribution that an energy exchange between the molecule and solid (which may eventually yield desorption or dissociation) becomes possible. The first contribution to these "bond potential energies" may then be modeled by some analytical potential formulas such as a harmonic well, a Morse potential, or other suggested potential formulas. The rest of $\epsilon_e(\vec{R})$, i.e., that part which can be identified with the solid coordinates, may then be replaced by a certain model of the solid [remember that internuclear interactions were included in $\epsilon_e(\vec{R})$].

The corresponding nuclear-motion equations (2.4) may then be solved with the above-mentioned model replacement for $\epsilon_e(\vec{R})$, and their solutions provide the vibrational spectrum for the modeled system.

B. Coupling

In this section we derive, under certain approximations, an expression for the coupling between a point charge (of charge $+Z_A^*e$, where Z_A^* is the effective charge of the ion) adsorbed at a distance z_1 from a metal surface and the ***fluctuating*** part of the metal substrate. As discussed previously, in the model in which we develop the role of the electronic (including direct nuclear interactions) energy is to establish a bounded molecule-solid system characterized by, for example, a Morse potential with an equilibrium distance d_1 of the atomic constituents from the surface, with an associated manifold of vibrational levels.

To make the calculation tractable and yet preserving the essential physical features, we model the surface in the following manner. We consider an electron gas bounded by an infinite potential barrier (Fig. 1). The *static* ions are then placed within this potential and the first plane is positioned at a distance $L-z_0$ with $z_0\to 0$ from the potential barrier, where L is the linear dimension of the slab.

We now relax the static ions and allow them to fluctuate by emitting phonons. Denoting such a density fluctuation of the ions as $\delta n_b(\vec{r})$ and the electronic response to such a fluctuation as $\delta n_e(\vec{r})$, the coupling may be written as

$$v(\vec{r}) = \delta u_b(\vec{r}) + \delta u_e(\vec{r}) \,,$$

where $\delta u_b(\vec{r})$ and $\delta u_e(\vec{r})$ are the fluctuating ionic and electronic interaction potentials with the adsorbed charge $(+Z_A^* e)$ positioned at $\vec{r}$; i.e.,

$$\delta u_b(\vec{r}) = Z_A^* Z_s e^2 \int \frac{d\vec{r}\,'\delta n_b(\vec{r}\,')}{|\vec{r} - \vec{r}\,'|} \,, \tag{2.6}$$

$$\delta u_e(\vec{r}) = - Z_A^* Z_s e^2 \int \frac{d\vec{r}\,'\delta n_e(\vec{r}\,')}{|\vec{r} - \vec{r}\,'|} \,, \tag{2.7}$$

with Z_A^* and Z_s and atomic charges (possibly screened) of the adatom and metal ions, respectively. The position vector $\vec{r}$ of the point charge is set equal to $z_1 + L$ in Eqs. (2.6) and (2.7), where L is the thickness of the sample (Fig. 1). We choose next a wave vector $\vec{q}$ of the fluctuating ionic background and express the single Fourier component of the density fluctuation as

$$\delta n_b(z, \vec{r}_\parallel) = \delta n_b(q_\perp, \vec{q}_\parallel) \times \exp[i(q_\perp z + \vec{q}_\parallel \cdot \vec{r}_\parallel)] + \text{c.c.} \tag{2.8}$$

In the following we omit writing explicitly the parallel components $\vec{r}_\parallel$, $\vec{q}_\parallel$ from δn_b due to translational invariance in planes parallel to the surface, and denote $\delta n_b(z) \equiv \delta n_b(z, \vec{r}_\parallel)$ and $\delta n_b(q_\perp) \equiv \delta n_b(q_\perp, \vec{q}_\parallel)$. It is convenient to define an extension of $\delta n_b(z)$ (see below) by an even function $\delta n_b'(z)$ such that for z in the range $(-L, 0)$, $\delta n_b'(z) = \delta n_b(-z)$.

The potential $v(\vec{r})$ (for $\vec{r} = z_1 + L$) can be evaluated yielding

$$\begin{aligned} v(z_1 + L) &= Z_A^* Z_s e^2 \int d\vec{r}\,'_\parallel \int_0^L dz' \left(\frac{\delta n_b'(\vec{r}\,')}{|z_1 + L - \vec{r}\,'|} - \frac{\delta n_e'(\vec{r}\,')}{|z_1 + L - \vec{r}\,'|} \right) \\ &= 2\pi Z_A^* Z_s e^2 e^{-q_\parallel z_1} \left(\frac{\delta n_b'(q_\perp)}{q_\perp^2 + q_\parallel^2} - \sum_{k_\perp} \frac{1}{k_\perp^2 + q_\parallel^2} \, \delta n_e'(k_\perp) \right) . \end{aligned} \tag{2.9}$$

[In Eq. (2.9) we have neglected exponential terms like e^{-L} and also recall that, e.g., $\delta n_e'(k_\perp) \equiv \delta n_e'(k_\perp, \vec{q}_\parallel)$.] Note that the sum over $k_\perp$ in Eq. (2.9) reflects the fact that the electronic charge density responds with all $k_\perp$ values to the single Fourier component of the background fluctuation in Eq. (2.8).

Our final task is to evaluate the sum over $k_\perp$ in Eq. (2.9). To do that we treat the electrons semiclassically, which amounts to solving the linearized static collisionless Boltzmann equation[30,31]

$$\frac{\vec{p}}{m} \cdot \frac{\partial}{\partial \vec{r}} \delta f(\vec{p}, \vec{r}) = \frac{\partial}{\partial \vec{p}} f_0(\epsilon_{\vec{p}}) \cdot \frac{\partial}{\partial \vec{r}} \delta u(\vec{r}) \,, \tag{2.10}$$

where $\epsilon_p = p^2/2m$, $f_0(\epsilon_p)$ is the Fermi-Dirac distribution function and $\delta u(\vec{r})$ the self-consistent field given by Eqs. (2.6) and (2.7) (with Z_A^* omitted).

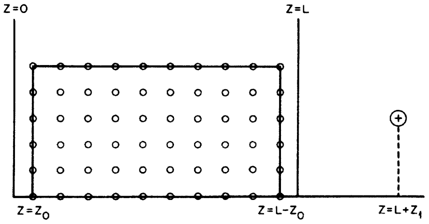

FIG. 1. Model adsorption system. The electron gas is bounded in a slab of linear dimension L. The first plane of substrate ions is located at $z = L - z_0$ with $z_0 \to 0$. The adsorbed ion is located at $z = L + z_1$.

The electron density $\delta n_e(\vec{r})$ is given by

$$\delta n_e(\vec{r}) = \int \frac{d^3 p}{(2\pi)^3} f(\vec{p}, \vec{r}) \,. \tag{2.11}$$

The boundary conditions dictated by the infinite barrier at the surface are those of specular reflection.

$$\delta f(p_\perp, z = 0, L) = \delta f(-p_\perp, z = 0, L) \,. \tag{2.12}$$

The solution of Eqs. (2.10)–(2.12) is not difficult[31] and we present in the following only the key relationships. It is convenient to extend the definition of Eq. (2.10) to the range $(-L, L)$ by defining the primed quantities $\delta u'(z)$, $\delta f'(p_\perp, z), \ldots$ as even function extensions of $\delta u(z)$, $\delta f(p_\perp, z), \ldots$. A Fourier transformation of Eq. (2.10) yields

$$\delta f'(p_\perp, k_\perp) = \frac{\partial f_0(\epsilon_p)}{\partial \epsilon_p} \delta u'(k_\perp) \,, \tag{2.13}$$

where

$$\delta f'(p_\perp, k_\perp) \equiv \frac{1}{2L} \int_{-L}^{L} dz \, e^{ik_\perp z} \delta f'(p_\perp, z) \tag{2.14}$$

and

$$k_\perp = n\pi/L \,, \quad n = 0, \pm 1, \pm 2, \ldots \,.$$

$\delta u'(k_\perp)$ can be easily derived from the even extension of Eqs. (2.6) and (2.7) and is given as

$$\delta u'(k_\perp) = \delta u'_b(k_\perp) + \bar{v}(k_\perp)\delta n'_e(k_\perp) - \frac{q_\parallel \bar{v}(k_\perp)}{L} \sum_{k'_\perp}{}' \frac{\delta n'_e(k'_\perp)}{k'^2_\perp + q^2_\parallel}\,, \tag{2.15}$$

where $\bar{v}(k_\perp) \equiv 4\pi e^2/(k^2_\perp + q^2_\parallel)$ and the sum over $k'_\perp$ is over even integers if $k_\perp$ is even and odd integers if $k_\perp$ is odd. We note from Eqs. (2.13)–(2.15) that the solution of Eq. (2.13) satisfies the specular reflection boundary condition automatically which was the motivation underlying the extension of the functions from $-L$ to 0. Integrating both sides of Eq. (2.13) over $\vec{p}$ and using Eq. (2.15) for $\delta u'(k_\perp)$ gives the following self-consistent equation for $\delta n'_e(k_\perp)$:

$$[1 + \bar{v}(k_\perp)N(0)]\,\delta n'_e(k_\perp) = -N(0)\delta u'_b(k_\perp) + \bar{v}(k_\perp)N(0)\frac{q_\parallel}{L}\sum_{k'_\perp}{}' \frac{\delta n'_e(k'_\perp)}{k'^2_\perp + q^2_\parallel}\,, \tag{2.16}$$

where the density of states at the Fermi level $N(0)$ is

$$N(0) = -\int \frac{\partial f_0(\epsilon_p)}{\partial \epsilon_p}\frac{d^3p}{(2\pi)^3}\,.$$

Dividing both sides of Eq. (2.16) by $1 + \bar{v}(k_\perp)N(0)$, multiplying by $(k^2_\perp + q^2_\parallel)^{-1}$, and summing over $k_\perp$, we can finally solve for the restricted sum over $k'_\perp$ to give the final form

$$\delta n'_e(k_\perp) = -\frac{N(0)}{1 + N(0)\bar{v}(k_\perp)}\left(\delta u'_b(k_\perp) + \frac{q_\parallel N(0)\bar{v}(k_\perp)}{DL}\sum_{k'_\perp}{}' \frac{1}{1 + N(0)\bar{v}(k'_\perp)}\frac{\delta u'_b(k'_\perp)}{k'^2_\perp + q^2_\parallel}\right), \tag{2.17}$$

where

$$D = 1 - \frac{q_\parallel}{L}\sum_{k'_\perp}{}' \frac{N(0)\bar{v}(k'_\perp)}{(k'^2_\perp + q^2_\parallel)[1 + N(0)\bar{v}(k'_\perp)]}$$
$$= 1 - \frac{\lambda^2_{\mathrm{TF}}}{2(q^2_\parallel + \lambda^2_{\mathrm{TF}})^{1/2}[q_\parallel + (q^2_\parallel + \lambda^2_{\mathrm{TF}})^{1/2}]} \tag{2.18}$$

where

$$\lambda^2_{\mathrm{TF}} = 4\pi e^2 N(0)\,,$$

$$\delta u'_b(k_\perp) = \frac{4\pi e^2}{q_\parallel}\delta n_b(q_\perp) \times\left(\frac{q_\parallel}{q^2_\perp + q^2_\parallel}\delta_{q_\perp, k_\perp} - \frac{q^2_\parallel}{L(q^2_\perp + q^2_\parallel)(q^2_\parallel + k^2_\perp)}\right) \tag{2.19}$$

and TF represents Thomas-Fermi. Substituting Eq. (2.19) in Eq. (2.17), the sum over $k_\perp$ in Eq. (2.9) may now be evaluated yielding our final expression for $v(z_1 + L)$:

$$v(z_1 + L) \equiv v(z_1) = \frac{Z^*_A Z_s e^2 2\pi \delta n_b(q_\perp)\exp(-q_\parallel z_1)}{(q^2_\perp + q^2_\parallel)D} \times\left(1 - \frac{\lambda^2_{\mathrm{TF}}}{q^2_\perp + q^2_\parallel + \lambda^2_{\mathrm{TF}}}\right). \tag{2.20}$$

Within the context of the infinite surface barrier as a model for the static semi-infinite crystal the generalization of Eq. (2.20) to include crystallinity of the substrate would involve simply treating $\delta n_b(q_\perp, \vec{q}_\parallel)$ in terms of the phonon crystal propagator. In the present calculation we, however, would use a continuum Debye model of the solid.

In a continuum model of the solid the Fourier components of the positive background number-density fluctuations, $\delta n_b(\vec{q})$ see Eq. (2.8), are defined by the relation

$$\delta n_b(\vec{r}) = \sum_{\vec{q}} \delta n_b(\vec{q})e^{i\vec{q}\cdot\vec{r}} \tag{2.21}$$

and $\delta n_b(\vec{r})$ is given as[31]

$$\delta n_b(\vec{r}) = -Z_s n_0 \vec{\nabla}\cdot\vec{D}\,, \tag{2.22}$$

where n_0 is the ionic number density of the solid and $\vec{D}$ is the displacement of the background from its equilibrium position. From Eqs. (2.21) and (2.22) it follows that

$$\delta n_b(q_\perp, \vec{q}_\parallel) \equiv \delta n_b(q_\perp) = Z_s n_0\left(\frac{\hbar}{2M_s n_0 \Omega \omega_{\vec{q}}}\right)^{1/2} q(b_{\vec{q}} + b^\dagger_{-\vec{q}})\,, \tag{2.23}$$

where M_s is the atomic mass of a solid atom, Ω is the volume of the solid, and $b_{\vec{q}}$ ($b^\dagger_{\vec{q}}$) are the annihilation (creation) operators of a phonon of wave vector $\vec{q}$ and frequency $\omega_{\vec{q}}$. We now express the instantaneous position of the adsorbed atom z_1 as $z_1 = d_1 + u_1$, where d_1 is the equilibrium distance of the atom from the surface, and expand the exponent in Eq. (2.20) as

$$e^{-q_\parallel z_1} = e^{-q_\parallel d_1}(1 - q_\parallel u_1 + \tfrac{1}{2}q^2_\parallel u^2_1 + \cdots)\,. \tag{2.24}$$

Substitution of Eqs. (2.23) and (2.24) into Eq. (2.20) yields an expression for $v(z_1)$, which may be written as

$$v(z_1) = v_0(\vec{q};d_1) + \delta v_1(\vec{q};u_1) + \delta v_2(\vec{q};u_1) + \cdots\,, \tag{2.25}$$

$$\delta v_1(\vec{q};u_1) = g^{(1)}_{\vec{q}} u_1(b_{\vec{q}} + b^\dagger_{-\vec{q}})\,, \tag{2.26a}$$

$$\delta v_2(\vec{q};u) = g^{(2)}_{\vec{q}} u^2_1(b_{\vec{q}} + b^\dagger_{-\vec{q}})\,, \tag{2.26b}$$

where $\delta v_1(\vec{q};u_1)$ is the potential corresponding to bilinear coupling between the vibrations of the atom and the phonons of the solid. Assuming for simplicity an acoustic continuum model for the solid, i.e., $\omega_q = sq$, where s is the sound velocity, $g^{(1)}_{\vec{q}}$ in Eq. (2.26) is given by

$$g_q^{(1)} = -F\frac{q^{1/2}q_{\parallel}}{q^2+\lambda_{\mathrm{TF}}^2}\left(1+\frac{\lambda_{\mathrm{TF}}^2}{2(q_{\parallel}^2+\lambda_{\mathrm{TF}}^2)^{1/2}[q_{\parallel}+(q_{\parallel}^2+\lambda_{\mathrm{TF}}^2)^{1/2}]-\lambda_{\mathrm{TF}}^2}\right)e^{-q_{\parallel}d_1}, \tag{2.27a}$$

where

$$F = 2\pi Z_s Z_A^* e^2\left(\frac{\hbar n_0}{2M_s\Omega s}\right)^{1/2}. \tag{2.27b}$$

The above derivation of the vibrational coupling can be applied to any of the atoms of the molecule which interacts with the surface by simply using the appropriate effective atomic charge Z_A^* and equilibrium distance d_1. For the sake of simplicity, we will limit ourselves in the following to a single adsorbed atom (the extension to a polyatomic molecule is easy and will be presented elsewhere). Our results can be summarized by writing the Hamiltonian for our model system as

$$H = \epsilon_e^0 + H_v^0 + H', \tag{2.28a}$$

$$H' = \sum_i v(z_i), \tag{2.28b}$$

[the index i in Eq. (2.28b) simply generalizes our coupling to several adsorbates] where ϵ_e^0 is the electronic energy (including direct nuclear-nuclear interactions) for equilibrium nuclear positions and H_v^0 is the zeroth-order Hamiltonian for the adsorption system

$$H_v^0 = \sum_{\vec{q}} \hbar\omega_{\vec{q}}(b_{\vec{q}}^{\dagger}b_{\vec{q}}+\tfrac{1}{2}) + \sum_m H_{v,m}, \tag{2.29}$$

where the first term on the right corresponds to the harmonic solid (and in our model a Debye model is employed), and the second term corresponds to the vibrational energies of intramolecular and chemisorptive bonds (the m summation extends over all bonds). The last term [Eq. (2.28b)] in Eq. (2.28a) contains couplings between the vibrations of intramolecular and chemisorptive bonds and fluctuations in the solid, see Eqs. (2.25)–(2.27). We note that in a more refined description local modes due to the adsorbate could be included.

C. Transition rate

The final quantity which we require before turning to the stochastic evolution of the system (see Sec. III) is the transition rate between vibrational levels of the adsorbed system. These transitions occur due to the coupling Hamiltonian H' in Eq. (2.28a). To lowest order in perturbation theory the transition rates can be calculated by the golden-rule formula[32]

$$W_{v\to v'} = \frac{2\pi}{\hbar}\sum_{n_q,n_q'} p(n_q)\,|\langle v',n_q'|H'|v,n_q\rangle|^2 \times \delta(\epsilon_{v'}-\epsilon_v+\epsilon_{n_q'}-\epsilon_{n_q}), \tag{2.30}$$

where we sum over phonon final states n_q' and average over phonon initial states n_q using the probability distribution $p(n_q)$.

In order to evaluate $W_{v\to v'}$ we need to specify the manner in which we model the vibrational spectrum of the adsorbed molecule.

(i) In the crudest approximation the vibrations are modeled by harmonic oscillators, truncated at the appropriate predissociation levels (see Sec. III). Keeping only terms up to bilinear coupling [δv_1, see Eq. (2.25)] allows only for single quantum transition ($v\to v\pm 1$), accompanied by the absorption (emission) of a phonon. Denoting the harmonic frequency by ω_0, δv_1 in Eq. (2.26a) can be written as

$$\delta v_1(\vec{q}) = g_{\vec{q}}^{(1)}\left(\frac{\hbar}{2\omega_0 M_A}\right)^{1/2}(a+a^{\dagger})(b_{\vec{q}}+b_{-\vec{q}}^{\dagger}), \tag{2.31}$$

where M_A is the mass of the adsorbed atom and $a(a^{\dagger})$ are creation (annihilation) operators of the harmonic-oscillator states. Substitution of Eq. (2.31) in Eq. (2.30) yields for the transition rate between levels

$$W_{v\to v+1} = \frac{2\pi}{\hbar}\left(\frac{\hbar}{2\omega_0 M_A}\right)(v+1) \times \sum_{\vec{q}} |g_{\vec{q}}^{(1)}|^2\bar{n}_{\omega_{\vec{q}}}\delta(\hbar\omega_{\vec{q}}-\hbar\omega_0), \tag{2.32}$$

where the phonon occupation number is given by $\bar{n}_{\omega_{\vec{q}}} = [\exp(\beta\hbar\omega_{\vec{q}})-1]^{-1}$, $\beta=(k_BT)^{-1}$. For an isotropic Debye model of the solid, i.e., $\omega_q = sq$, and a cutoff frequency ω_D given by $\hbar\omega_D = \hbar s q_D = k\Theta_D$ where Θ_D is the Debye temperature, we replace the summation over $\vec{q}$ by an integral. Using the energy-conservation Dirac delta function and cylindrical coordinates the integration is straightforward, yielding

$$\frac{W_{v\to v+1}^{(h)}}{v+1} \equiv A(\omega_0) = \frac{3\pi^3e^4(Z_A^*Z_s)^2n_0^2\lambda_{\mathrm{TF}}^4}{M_AM_s\omega_D^3(q_0^2+\lambda_{\mathrm{TF}}^2)^2}\,\bar{n}_{\omega_0}(J_1+J_2+J_3), \tag{2.33a}$$

$$J_1 = \int_0^{\delta} x^3\exp(-2\lambda_{\mathrm{TF}}d_1x)\,dx, \tag{2.33b}$$

$$J_2 = 2\int_0^{\delta} x^3\exp(-2\lambda_{\mathrm{TF}}d_1x)/[1+2x^2+2x(x^2+1)^{1/2}]\,dx, \tag{2.33c}$$

$$J_3=\int_0^{\delta} x^3\exp(-2\lambda_{\mathrm{TF}}d_1x)/\{1-4[1+x^2+x(x^2+1)^{1/2}]+4(1+x^2)[1+2x^2+2x(x^2+1)^{1/2}]\}\,dx\,, \tag{2.33d}$$

where equal sound velocities for transverse and longitudinal modes have been used, $\delta=q_{D\parallel}/\lambda_{\mathrm{TF}}$, ($q^2_{D\parallel}=\frac{2}{3}q^2_D$), and $sq_0=\omega_0$. The integrals J_2 and J_3 are easily computed by numerical quadrature. The superscript (h) in $W^{(h)}_{v\to v+1}$ is introduced in reference to the harmonic-oscillator model. An analysis of the dependence of the transition rate $W^{(h)}_{v\to v+1}$ [Eq. (2.33a)] on characteristics of the adsorption system is presented below.

(ii) As an improved model of the bond potential energy between an adsorbed atom and the surface, we consider the Morse potential[33]

$$\epsilon_e(z-d_1)=D_e\{1-\exp[-\beta(z-d_1)]\}^2-D_e\,, \tag{2.34}$$

where D_e is the dissociation energy referred to the minimum, d_1 the equilibrium distance of the adsorbed atom from the surface, and the parameter β determines the width of the potential. One often defines the anharmonicity parameter $x_e=\hbar\omega_0/4D_e$ where ω_0 is the vibrational frequency for infinitesimal amplitudes (x_e is often determined empirically). The eigenvalues of the one-dimensional Schrödinger equation with the Morse potential are given by[34,35]

$$\epsilon_v=\hbar\omega_0(v-x_ev^2)-D_e\,, \tag{2.35}$$

and therefore the vibrational level spacing is

$$\Delta\epsilon_{v+1,v}=\hbar\omega_0[1-x_e(2v+1)]\,. \tag{2.36}$$

Using Eq. (2.30) for $W_{v\to v'}$ with H' given by Eqs. (2.28b), (2.25), and (2.26a), i.e., to linear order in u_1 (the derivation of the bond length from equilibrium), we observe that we need to compute the matrix elements $|\langle v'|u_1|v\rangle|^2$, where $|v\rangle$ is the Morse eigenfunction corresponding to ϵ_v in Eq. (2.35). These matrix elements have been calculated by several authors.[35,36] While the results given in Eqs. (21)-(24) of Ref. 35 are valid for all v,v' we will be interested only in nearest and next-nearest level transitions, i.e., $v\to v\pm1$ and $v\to v\pm2$. In addition the expressions simplify significantly in the approximation $(v'+v'')x_e\ll1$, yielding[36]

$$|\langle v+1|u_1|v\rangle|^2=(d_1B_e/\omega_0)(v+1)[1+x_e(1+v)] \tag{2.37}$$

$$|\langle v+2|u_1|v\rangle|^2=(d_1^2B_ex_e/4\omega_0)(v+1)(v+2). \tag{2.38}$$

The expression for the transition rate between Morse levels v and v' can now be written as

$$W^{(M)}_{v\to v'}=\frac{2\pi}{\hbar}\sum_{\vec q}|g^{(1)}_{\vec q}|^2\bar n_{\omega_{\vec q}}|\langle v'|u_1|v\rangle|^2\times\delta(\epsilon_{v'}-\epsilon_v-\hbar\omega_{\vec q})\,. \tag{2.39}$$

Using the matrix elements given by Eqs. (2.37) and (2.38) and the Debye model for the solid we obtain to first order in the anharmonicity x_e the following expressions for $v'=v+1$ and $v+2$,

$$\frac{W^{(M)}_{v\to v+1}}{v+1}=A(\omega_0)\{1+x_e[(v+1)-(2v+1)B(\omega_0)]\}\,, \tag{2.40}$$

where

$$B(\omega_0)=\frac{\omega_0}{A(\omega_0)}\frac{\partial A(\omega_0)}{\partial\omega_0} \tag{2.41}$$

and

$$\frac{W^{(M)}_{v\to v+2}}{(v+1)}=\tfrac{1}{4}x_e(v+1)(v+2)A(2\omega_0)\,, \tag{2.42}$$

where $A(\omega_0)$ is given in Eq. (2.33).

To demonstrate the dependence of the transition rates between vibrational levels on the model of the potential well, the temperature and characteristics of the adsorption system such as the equilibrium distance and fractional charge on the atom, we present the numerical evaluation of Eqs. (2.33) and (2.34) in Figs. 2-4. In Fig. 2, the variation of $W_{v\to v'}$ for potassium adsorption on tungsten,[37] with temperature and model potential is displayed. The differences between the results using harmonic and Morse potentials are evident. Note that for the Morse potential $W_{1\to2}\gg W_{1\to3}$. In addition the transition rates between high-lying vibrational levels in the Morse potential are much larger than between the bottom-lying levels. This indicates that transitions between the low-lying levels may be the bottle neck in the incoherent multiphonon evolution of the system (see Sec. III). The marked dependence of the transition rates on temperature should also be noted, and is associated with the temperature-dependent phonon occupation number $\bar n_{\omega_q}$.

Similar dependences are seen for xenon adsorbed on tungsten[38-40,9] (Fig. 3) where in addition the sensitivity to the equilibrium distance d_1 and fractional charge on the atom are demonstrated. Finally, in Fig. 4, $W^{(M)}_{v\to v+1}$ as a function of the level number v for Xe/W system at $T=100$ K is shown to increase markedly. The influence of these results on the rates of desorption will be investigated in Sec. III.

III. EVALUATION OF FIRST PASSAGE TIMES FOR THE TRUNCATED-HARMONIC-OSCILLATOR AND MORSE-POTENTIAL MODELS

Having obtained explicit expressions for the couplings between the adsorbate and the substrate

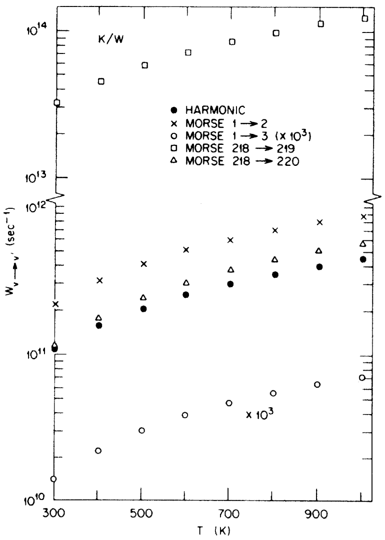

FIG. 2. Transition rate ($W_{v\to v'}$) vs temperature for potassium adsorbed on tungsten. The parameter used in the calculation: fractional charge on the potassium $z_A^* = 0.27e$ and equilibrium distance of the adsorbate from the substrate, $d_1 = 2.38$ Å, were chosen after Ref. 37. The transition rate, $W_{v\to v+1}$, for a harmonic-well description of the chemisorption bond, is marked by solid dots, using a vibrational quanta $\hbar\omega_0 = 13.7$ meV [after L. M. Kahn and S. C. Ying, Solid State Commun. 16, 799 (1975)]. The rest are results of calculations employing a Morse-potential description, for $W_{1\to 2}^{(M)}$, $W_{1\to 3}^{(M)}$, $W_{218\to 219}^{(M)}$, and $W_{218\to 220}^{(M)}$, where $v = 220$ is the predissociation level. Note the change of scale in $W_{1\to 3}^{(M)}$. The Debye temperature of the substrate was taken as $\Theta_D = 220$ °K, the electron number density of the substrate was $n_e = 38\times 10^{22}\,\text{cm}^{-3}$ and $x_e = 6.5\times 10^{-4}$.

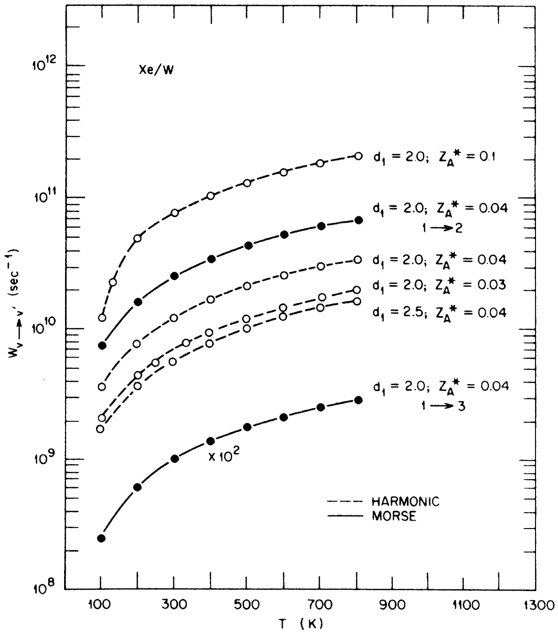

FIG. 3. Transition rates, $W_{v\to v'}$, using both harmonic (dashed) and Morse (solid line) potentials for Xe adsorbed on tungsten, vs temperature. The harmonic vibrational quanta $\hbar\omega_0$ was chosen as 3.0 meV. The sensitivity of the transition rates to variations in the equilibrium distance d_1 (in Å) and fractional charge on the adsorbed xenon are shown. The substrate parameters were taken as $\Theta_D = 220$ °K, $n_e = 38\times 10^{22}\,\text{cm}^{-3}$, and $x_e = 1.25\times 10^{-3}$.

and for the rates of transitions between vibrational levels of the binding potential, induced by the couplings, we turn next to the temporal evolution of the excitations. Since for most systems of interest the allowed quanta of excitation, dictated by the characteristics of the phonon spectrum of the substrate are much smaller than the barrier for bond rupture, an incoherent multiphonon mechanism is formulated. This, however, is applicable to systems in which the spacings between vibrational levels of the potential associated with the reaction coordinate do not exceed the maximum phonon frequencies. When the above is not satisfied coupling may occur through a mode other than the bond-rupture reaction coordinate which serves as a "doorway" state (see Sec. IV).

Consider an oscillator system with $x_n(t)$ the distribution describing the population of vibronic levels n at time t. The time evolution of this distribution is governed under certain approximations by a master equation[41]

$$-\frac{dx_n}{dt} = \sum_{\nu=0}^{N+1} W_{\nu n} x_n - \sum_{m=0}^{N} W_{nm} x_m, \quad n = 0, 1, \ldots, N \tag{3.1}$$

where N is the predissociation level, W_{nm} is the transition probability per unit time from m to n. In the above equation second-order terms due to recombination are neglected. The initial distribution ($t = 0$) is normalized according to

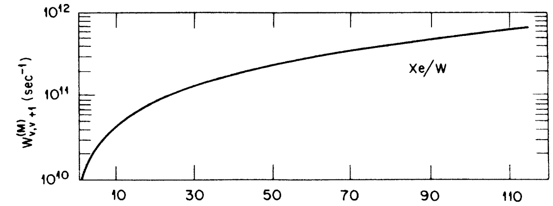

FIG. 4. Morse transition rate, $W_{v\to v+1}^{(M)}$ vs level number v, for Xe adsorption on tungsten, at $T = 100$ °K. The equilibrium distance was taken at $d_1 = 2.0$ Å and fractional[9] charge $z_A^* = 0.04e$. Note the monotonous increase in $W_{v\to v+1}^{(M)}$ as v increases. The substrate parameters are as given in the caption to Fig. 3.

$$\sum_{n=0}^{N} x_n(0) = 1\,, \tag{3.2}$$

and the $x_n(0)$'s are given by a Boltzmann distribution at temperature T; i.e.,

$$x_n(0) = e^{-\beta\epsilon_n} \sum_{n=0}^{N} e^{-\beta\epsilon_n}\,. \tag{3.3}$$

For the calculation of the reaction rate we will be interested in the mean time for the system specified above, to pass the Nth level for *the first time*—i.e., the *mean first passage time*, $\bar{t}$. The distribution of first passage times $P(t)$ is given by[41]

$$P(t) = -\frac{d}{dt}\sum_{n=0}^{N} x_n(t) \tag{3.4}$$

and $\bar{t}$ is the first moment of $P(t)$; i.e.,

$$\bar{t} = \int_0^\infty tP(t)dt\,. \tag{3.5}$$

An expression for the mean first passage time for an initial population distribution $x_n(0) = \delta_{n,0}$ for a truncated-harmonic-oscillator system and transitions between neighboring levels only, was first given by Montroll and Shuler.[41] This has been generalized by Kim[42] for the Boltzmann initial distribution [Eq. (3.3)] for both a truncated harmonic and Morse oscillators with nearest- and next-nearest-neighbor transitions.

(i) For the truncated harmonic oscillator the result is[42]

$$\bar{t}^{(h)} = \frac{(v+1)}{W^{(h)}_{v\to v+1}(1-e^{-\theta})} \sum_{j=1}^{N+1} j^{-1}(e^{j\theta}-1)(1-e^{-j\theta})\,, \tag{3.6}$$

with $\theta = \hbar\omega_0/kT$, where ω_0 is the harmonic-oscillator frequency.

(ii) To obtain an expression for the mean first passage time out of a Morse-potential well $\bar{t}^{(M)}$ with transitions between nearest and next-nearest levels, we adopt the methods developed by Kim. The generalization of Kim's result [Eqs. (6.15) and (6.16) of Ref. 42] amount to taking into account that in our case the exchange of excitation is with a solid characterized by thermal occupation numbers

$$\bar{n}_{\omega_q} = [\exp(\hbar\omega_q/kT) - 1]^{-1}\,.$$

Consequently contributions corresponding to transitions between the Morse-potential levels must be weighted appropriately. Starting from Eq. (6.6) of Ref. 42,

$$\bar{t}^{(M)} = \sum_{p=0}^{N} \frac{Q_p u_p}{D_p} - \sum_{p=0}^{N} Q_p\left(\frac{h_{p+1,p-1}}{D_pD_{p-1}}u_{p-1} + \frac{h_{p+2,p}}{D_p}\frac{u_{p+1}}{D_{p+1}}\right), \tag{3.7}$$

with Q_p, u_p, and D_p given by

$$Q_p = \sum_{n=0}^{p} e^{-\beta\epsilon_n}\,, \tag{3.8a}$$

$$u_p = \sum_{n=0}^{p} x_n(0) \tag{3.8b}$$

$$D_p = h_{p+1,p} + h_{p+2,p} + h_{p+1,p-1}\,, \tag{3.8c}$$

see Eqs. (4.13), (4.4), and (6.1) in Ref. 42, and the h_{mn} given explicitly by

$$\begin{aligned} h_{p+1,p} = {} & A(\omega_0)(p+1) \\ & \times \{1 + x_e[(p+1) \\ & - B(\omega_0)(2p+1)]\}e^{-\beta\epsilon_{p+1}}\,, \end{aligned} \tag{3.9a}$$

$$h_{p+2,p} = A(2\omega_0)(x_e/4)(p+1)(p+2)e^{-\beta\epsilon_{p+2}}\,, \tag{3.9b}$$

$$h_{p+1,p-1} = A(2\omega_0)(x_e/4)p(p+1)e^{-\beta\epsilon_{p+1}}\,, \tag{3.9c}$$

we obtain

$$\bar{t}^{(M)} = \bar{t}_0 + [x_e/A(\omega_0)]\,\bar{t}_1\,. \tag{3.10}$$

In Eq. (3.10)

$$\bar{t}_0 = \frac{1+a}{A(\omega_0)} \sum_{p=1}^{N+1} \frac{e^{\beta\epsilon_p}}{p}(1-e^{-p\theta})^2\,, \tag{3.11}$$

where $\theta = (\hbar\omega_0/kT)$, $A(\omega_0)$ is given by Eq. (2.33a), and $a = 1/(e^\theta - 1)$. $\bar{t}_1$ in the above equation is given by

$$\begin{aligned} \bar{t}_1 = {} & A(\omega_0)\bar{t}_0[a\theta(1+2a) + Z(\omega_0)/[4(1+a)] - B(\omega_0)] + e^{\beta\epsilon_{N+1}}\tfrac{1}{4}Z(\omega_0)[2 + a/(1+N) + 3a] \\ & - \sum_{p=1}^{N+1} e^{\beta\epsilon_p}[1 + a + \tfrac{1}{4}Z(\omega_0)(3+4a) - 2(1+a)B(\omega_0)] - N\theta(N+1)(1+a) \\ & + (2N-a)[1 + a + \tfrac{1}{2}Z(\omega_0)(1+2a) - 2(1+a)B(\omega_0)] + 2\theta a(1+a)(1+3a-2N) - \tfrac{1}{4}Z(\omega_0)(1+a)\,, \end{aligned} \tag{3.12}$$

where

$$Z(\omega_0) \equiv \frac{A(2\omega_0)}{A(\omega_0)} = \frac{\bar{n}_{2\omega_0}}{\bar{n}_{\omega_0}}\left(\frac{q_0^2 + \lambda_{\text{TF}}^2}{4q_0^2 + \lambda_{\text{TF}}^2}\right)^2 \tag{3.13}$$

and $sq_0 = \omega_0$.

In the stochastic formulation of nonequilibrium kinetics which we have employed, the reaction rate R is given by the inverse of the mean-first-passage time $\bar{t}$ (see also discussion in Sec. IV). Results for the rates of desorption of potassium and xenon from a tungsten substrate are shown in Figs. 5–7. In Fig. 5 results for the two models of the binding potential (harmonic—solid line, and Morse—dashed line) using experimentally[37] suggested values for the desorption energy $D_e = 2640$ meV, equilibrium distance $d_1 = 2.38$ Å and fractional charge $Z_A^* = 0.27e$ are compared, along with the experimentally obtained[34] rate, given by $R = 10^{12.8} \times \exp(-D_e/kT)$ (open circles). It is evident that the results for the Morse-potential and truncated-harmonic-oscillator models yield both an Arrhenius-like straight line in the semilogarithmic plot of R vs $1/T$. The pre-exponential factors, however, differ markedly with the Morse potential in agreement with experiment. It should be noted that the differences between the two models are less pronounced than those which were exhibited in the transition rates (see Figs. 2 and 3). Similar results, with a somewhat less pronounced difference between the two models and in agreement with experiment[38] are shown for xenon desorption from tungsten (with the parameters given in the figure captions) in Figs. 6 and 7. In Fig. 7 the rather weak dependence of the results for the rate of desorption on the equilibrium distance parameter is exhibited.

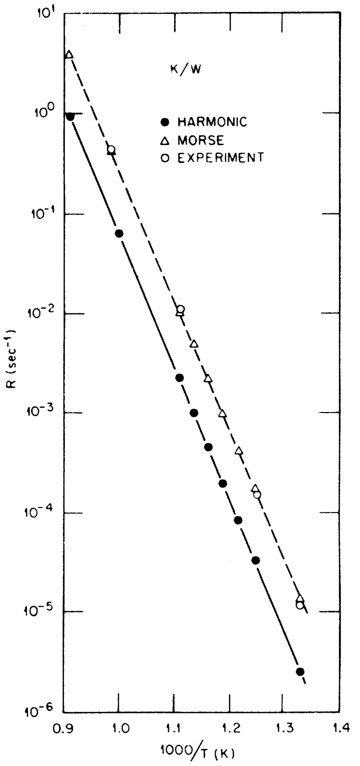

FIG. 5. Semilogarithmic plots of desorption rates vs inverse temperature for the system potassium adsorbed on tungsten. The desorption energy D_e was taken as 2.64 eV after Ref. 37, and the rest of the characteristic parameters are as given in the caption to Fig. 2. The experimental points (open circles) were taken after Ref. 37, $R(T) = 10^{12.8} \times \exp(-D_e/kT)$. Both the Morse potential (dashed) and truncated harmonic (solid) yield linear relationships in the plot of ln $R(T)$ vs inverse temperature, parallel to one another (same activation energy for desorption) but with different intercepts (frequency factors). The results based on the Morse-potential description of the chemisorptive bond are in better agreement with the experimentally deduced results than those derived from a truncated-harmonic potential.

IV. DISCUSSION AND PERSPECTIVES

We have formulated a theoretical model for the calculation of desorption rates of an adatom from a metal surface. The formulation relied on several key stages: (a) the evaluation of the coupling between the solid and the adatom induced by the

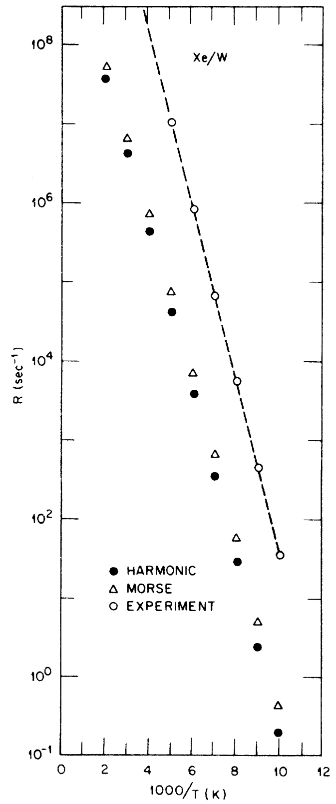

FIG. 6. Semilogarithmic plots of desorption rates $R(T)$ vs inverse temperature for the system xenon adsorbed on tungsten. The characteristic parameters are those given in the caption to Fig. 2 and the desorption energy D_e was taken as 217 meV after Ref. 38. The experimental points (open circles) were calculated from the rate expression given in the above reference $R(T) = 10^{12} \times \exp(-D_e/kT)$. Results obtained by using Morse (triangles) and truncated-harmonic potentials (dots) are shown.

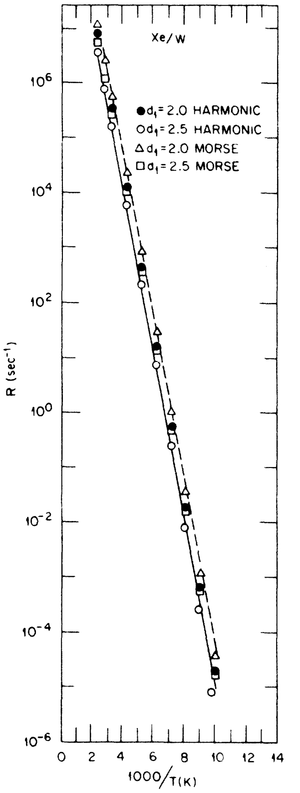

FIG. 7. Semilogarithmic plots of desorption rates $R(T)$ vs inverse temperature for Xe adsorbed on tungsten, characteristic parameters are as in Fig. 4 with $D_e = 300$ meV. Results are shown for both truncated-harmonic (solid and open dots) and Morse (triangles and squares) potentials. The apparent slight sensitivity of the rates to the equilibrium distance of the adsorbed atom from the surface is shown.

nonstationary substrate, (b) the stochastic incoherent multiphonon mechanism of excitation, and (c) the coupling to the final-state channels. From the results presented in Figs. 5–7, it is apparent that the model provides a rather adequate description of desorption for both weak (Xe/W) and strong (K/W) chemisorption systems. The principal merit of this model is that it exhibits explicitly the dependencies on various microscopic quantities characteristic to the substrate and adatom. Due to the complexity of the problem, our model relies on a number of simplifying assumptions certain of which we enumerate below: (a) the substrate was modeled as a continuum structureless solid, (b) surface phonons have been ignored, (c) the electron response to fluctuations of the ionic charge was calculated semiclassically (quantum interference effects neglected) and with specular boundary conditions imposed, (d) electronic band-structure effects were ignored which implies weak electron-ion coupling in the substrate, (e) bilinear coupling between the nonstationary adatom and substrate was used in the numerical examples and transition rates due to these couplings were calculated using the Fermi golden rule, and (f) an immobile adsorbate was assumed. The inclusion of adsorbate migration on the surface will add an entropy correction to the rate expression. While further improvements within this model are possible, the present study allows for a first evaluation of the sensitivity of desorption kinetics to the various microscopic parameters.

The standard approaches to reaction kinetics, such as absolute rate theory[2] (ART) and the various statistical methods[10] (e.g., RRKM) rely upon certain criteria of applicability. The main requirement of the above is that the initial and final (or transition complex) states are uncorrelated.[2] As discussed originally by Kramers[12] and further investigated recently,[13,14,43] the applicability of ART is related to the strength of the fluctuating part of the coupling (friction in the nomenclature of the above studies) between the adsorbate and the adparticle. The analytical results obtained[12] in the limits of small and large coupling support the assertion that the applicability of ART is limited to an intermediate regime of the coupling strength. In this regime the coupling is strong enough as to replenish instantaneously the equilibrium Maxmellian tail of particle momenta, necessary for surmounting the reaction barrier, and thus the rate becomes independent of the coupling. Outside this regime the Arrehnius behavior of the rate constant gets modified by multiplicative factors which vary with temperature. Our calculation of $\bar{t}$ [e.g., in Eq. (3.6)] in principle assumes the weak-coupling regime since our transition rates $W_{v\to v+1}$ are treated to lowest order in perturbation [e.g., Eq. (2.30)]. This assumption of weak coupling has internal consistency in that our low-order treatment does yield good agreement with experiment (Figs. 6 and 7). While clearly the interplay between the temperature dependence of $W_{v\to v+1}$ and the usual statistical occupations [the sum over j in Eq. (3.6)] is a complicated one and cannot rigorously reduce to an Arrehnius-like form our numerical results (displayed in Figs. 6 and 7) give a measure for the *weak* deviation from such a behavior. This conclusion cannot be inferred directly from the evaluated transition rates alone (Figs. 2–4) but requires an analysis of the rates. In this context it is important, however, to notice the dependence of the results on the model potential used (truncated-harmonic vs Morse potentials), and that the difference in rates of desorption corresponding to the two model potentials is smaller than that exhibited in the associated level transition probabilities.

The stochastic treatment of the time evolution of the vibrational excitations leading to desorption which we have used, is a convenient formulation of nonequilibrium kinetic processes. In the equilibrium theory the rate constant depends only upon transitions which couple bound vibrational levels directly to the dissociated state,[42] $N+1$, and similar to the basic assumption of ART there is no dependence on the details of the excitation mechanism. The first passage time $\bar{t}$ calculated via the stochastic nonequilibrium formulation does not in general equal the reciprocal of the equilibrium rate constant.[42] One limit in which the above equality holds is when the energy required for a transition is large compared to the available thermal energy. This condition was not obeyed in our cases. Thus, it was necessary to investigate the full stochastic behavior.

The order of coupling in our model should also be commented on. While we have used bilinear coupling [Eq. (2.26)], a generalization would in principle allow treatment of higher-order coupling terms. In this context we could argue that by a proper transformation of the coordinates $\{R_S\}$ and $\{R_M\}$ the bilinear coupling term could be removed and the frequencies of the substrate-adatom system renormalized accordingly. The coupling enters now through the new frequencies in these transformed canonical coordinates. It is now, *in principle* possible to calculate desorption rates with the simple assumption of a Boltzmann occupation of these new levels, and with proper retransformation of our coordinates to define the stage of dissociation. Such a calculation is expected to yield similar results to ours (particularly in the weak coupling limit) but it is rather complex and has not as yet been carried out for the model systems discussed in this study.

A detailed investigation of reaction mechanisms requires an analysis of the reaction products. Indeed a well-established practice in gas-phase kinetic studies[44] is to perform state-selective measurements, i.e., identification of products, their center-of-mass translational energies, and excitation of internal degrees of freedom. This mode of investigation is not common practice in current studies of surface reactions. In most, if not all, studies to date the experimental information consists only of mass, and in certain cases angular, distribution of the products. In the following we remark briefly on the possibility of *final-state branching* and suggest methods for its evaluation.

Having achieved the $(N+1)$th level, ϕ_{N+1}, whose energy E_{N+1} lies above the dissociation energy, the system may evolve via several channels. For example the ϕ_{N+1} state may decay into the translational continuum which corresponds to desorption, it may couple to a manifold of bound vibrational states associated with an excited electronic term or to a bound vibrational manifold or translation continuum corresponding to binding or diffusion along the surface. The problem is formally similar to that encountered in the study of autoionization[45] and predissociation[46-48,18] phenomena, and applied also to the study of radiationless transitions in molecules[49-51] and photodissociation[52-56] for which a number of methods of solution have been suggested. In the following we outline results obtained through the use of one of these methods.[45,49] Consider the case in which the excited vibrational state ϕ_{N+1} is embedded and coupled to two manifolds of states: (i) a manifold of bound vibrational states, $\{\psi_n\}$ associated with an excited electronic state of the adsorption system, (ii) a translational continuum, $\{\xi_E\}$. These two manifolds are assumed uncoupled to one another. Coupling of ϕ_{N+1} to $\{\psi_n\}$ is achieved via the nonadiabatic nuclear-kinetic-energy terms in the total Hamiltonian, and the corresponding matrix element will be taken as a constant v_1. The matrix element coupling ϕ_{N+1} to the translational continuum $\{\xi_E\}$ is denoted by v_2. The manifolds are normalized with $\langle \psi_n|H|\psi_j\rangle = \delta_{n,j}E_n$ and $\langle \xi_E|H|\xi_{E'}\rangle = E\delta(E-E')$. The configurational mixing of ϕ_{N+1} with the above final-state manifolds results in a stationary state Ψ_E, given by

$$\Psi_E = a(E)\phi_{N+1} + \sum_{n=-\infty}^{\infty} b_n(E)\psi_n + \int C_{E'}(E)\xi_{E'}dE' , \tag{4.1}$$

where the vibrational energies of the $\{\psi_n\}$ manifold are taken[49] as $E_n = E_{N+1} - \alpha + n\epsilon$, $n = 0, \pm 1, \pm 2 \ldots$ etc. and $\alpha = E_{N+1} - E_0$.

The probabilities for finding the system in the vibrational manifold $\{\psi_n\}$, $P_r(t)$, for remaining in ϕ_{N+1}, $P_d(t)$ and for being in the translational continuum, $P_f(t)$, are given by[52]

$$P_r(t) = \sum_{n=-\infty}^{\infty} \left| \int_{-\infty}^{\infty} dE\, e^{-(iE/\hbar)(t-\bar{t})} a^*(E) b_n(E) \right|^2 , \tag{4.2a}$$

$$P_d(t) = \left| \int_{-\infty}^{\infty} dE\, e^{-(iE/\hbar)(t-\bar{t})} |a(E)|^2 \right|^2 , \tag{4.2b}$$

$$P_f(t) = \int_{-\infty}^{\infty} dE' \left| \int_{-\infty}^{\infty} dE\, e^{-(iE/\hbar)(t-\bar{t})} a^*(E) C_{E'}(E) \right|^2 , \tag{4.2c}$$

where $\bar{t}$ is the mean first passage time calculated in Sec. III, i.e., the mean time for "preparation" of the system in state ϕ_{N+1}. In addition $P_d + P_r + P_f = 1$. Using the by now standard methods[45,51] with the appropriate scattering boundary conditions closed form approximate solutions can be obtained in the "statistical limit,"[50] i.e., for time t, such that $\tau \equiv t - \overline{t} \ll \hbar/\epsilon$,

$$P_r(\tau) = \frac{|v_1|^2}{|v_1|^2 + \epsilon |v_2|^2} (1 - e^{-\tau/\Gamma}) , \tag{4.3a}$$

$$P_d(\tau) = \exp(-\tau/\Gamma) , \tag{4.3b}$$

$$P_f(\tau) = 1 - P_d(\tau) - P_r(\tau) , \tag{4.3c}$$

$$\Gamma = (\hbar\epsilon/2\pi)(|v_1|^2 + \epsilon |v_2|^2)^{-1} . \tag{4.3d}$$

If the decay into the final states is fast the above expressions allow us to follow the reaction through its evolution. It is seen from Eqs. (4.3c), (4.3a), and (4.3b) that the average lifetime of the ϕ_{N+1} state is given by Γ where Γ is given by Eq. (4.3d). Thus, if a two-step process is postulated, i.e., preparation of the excited ϕ_{N+1} state followed by coupling to final states, the total rate of desorption is $R = (\overline{t} + \Gamma)^{-1}$. The probabilities given by Eqs. (4.3) could be used for the elucidation of the reaction products. The task of evaluating the matrix elements v_1 and v_2 which determine the magnitudes of the above quantities is the subject of further investigation. In particular we should note that in our results transverse motions of the adsorbates have not been considered. In a classical sense such motions would correspond to activated diffusion of the adsorbate near saddle point of the Born-Oppenheimer potential surface. Associated with these motions is an activation entropy which would modify the value of the rate constant. Indeed recent data for the desorption of CO from metals shows pre-exponential factors much larger than previously measured.[57]

Finally we comment on the application of our model to adsorbed molecular species. These systems possess additional degrees of freedom certain of which are of bond-stretching character and others which describe bond-bending, wagging, etc. While the energies typical to molecular bond-stretching modes might (and often do) exceed in magnitude those of single-phonon excitation by the solid, the energies associated with the non-stretching modes are smaller. Consequently it is suggested that the latter modes through their coupling to the vibrations of the solid may be excited up to high levels via an incoherent multiphonon mechanism similar to that used in the present investigation and subsequently couple via anharmonicity to the high-lying, densely spaced levels of the bond-stretching modes. Once these high-lying levels have been populated, the excitation may propagate further via direct coupling to the substrate, eventually leading to fragmentation (see Fig. 8). In other words the nonstretching modes may serve as doorway states[58] towards bond rupture via intramolecular energy redistribution.[57,56] Quantitative studies of this model of admolecule desorption and dissociation are in progress.

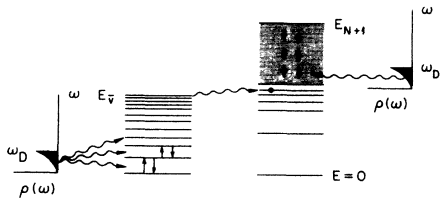

FIG. 8. Schematic picture of the door way-state model for thermal surface desorption or dissociation reaction mechanism. A characteristic Debye phonon density of states $\rho(\omega)$ is shown on the left and right. Excitation of a low-frequency, doorway, mode of vibration (typically a nonstretching mode) occurs via an incoherent multiphonon mechanism. Upon achieving the level $E_{\overline{v}}$ the excitation is transferred to the high-lying levels of a stretching mode (or comibnation of such modes) via anharmonic coupling. Further excitation in the dense vibrational manifold corresponding to the bond-rupture coordinate can occur via direct incoherent multiphonon excitations induced by thermal coupling to the substrate. The predissociation level is denoted by E_{N+1}. Having achieved this level the reaction proceeds through coupling to possible final-state channels such as dissociation, desorption, or migration.

ACKNOWLEDGMENTS

Useful conversations at the early stages of this study by W. Plummer, T. Madey, and R. Fox and comments on the manuscript by T. Kaplan are gratefully acknowledged. This work was supported by USDOE under Contract No. EG-77-S-05-5489 and by the Division of Materials Science under Contract No. W-7405-eng-26 with the Union Carbide Corporation.

---

[1] M. Boudart, in *Physical Chemistry: An Advanced Treatise*, Vol. VII, edited by H. Eyring (Academic, New York, 1975) Chap. 7; K. J. Laidler, *Reaction Kinetics* (Pergamon, New York, 1963), Vols. 1 and 2.

[2] S. Gladsstone, K. J. Laidler, and H. Eyrig, *The Theory of Rate Processes* (McGraw-Hill, New York, 1941).

[3] L. S. Kassel, *The Kinetics of Homogeneous Gas Reactions* (The Chemical Catalog Co., New York, 1932).

[4] H. S. Johnston, *Gas Phase Reaction Rate Theory* (Ronald, New York, 1966).

[5] D. O. Hayward and B. M. Trapnell, *Chemisorption* (Butterworths, London, 1964).

[6] R. Gomer, Adv. Sol. Stat. Phys. 30, 94 (1975).

[7] C. G. Goymour and D. A. King, J. Chem. Soc. Faraday Trans. 1, 68, 280 (1972).

[8] A. K. Mazumdar and H. W. Wassmuth, Surf. Sci. 30, 617 (1972).

[9] M. J. Dresser, T. E. Madey, and J. T. Yates, Jr., Surf. Sci. 42, 533 (1974).

[10] P. J. Robinson and K. A. Holbrook, *Unimolecular Reactions* (Wiley-Interscience, London, 1972); W. Frost, *Theory of Unimolecular Reactions* (Academic, New York, 1973).

[11] D. L. Bunker, *Theory of Elementary Gas Reaction Rates* (Pergamon, New York, 1966); W. L. Hase, in *Dynamics of Molecular Collisions*, Part B, edited by W. H. Miller (Plenum, New York, 1976).

[12] H. A. Kramers, Phys. Fenn. 7, 284 (1940).

[13] (a) H. Suhl, J. H. Smith, and P. Kumar, Phys. Rev. Lett. 25, 1442 (1970); (b) E. G. d'Agliano, W. L. Schaich, P. Kumar, and H. Suhl, in *Collective Properties of Physical Systems*, 24th Nobel Symposium 1973 (Academic, New York, 1974), p. 200; (c) E. G. d'Agliano, P. Kumar, W. Schaich, and H. Suhl, Phys. Rev. B 11, 2122 (1973).

[14] P. B. Visscher, Phys. Rev. B 13, 3272 (1976); 14, 347 (1976).

[15] G. Iche and P. Nozières, J. Phys. 37, 1313 (1976).

[16] N. B. Slater, *Theory of Unimolecular Reactions* (Methuen, London, 1959).

[17] N. Rosen, J. Chem. Phys. 1, 319 (1933).

[18] O. K. Rice, J. Chem. Phys. 55, 439 (1971); 1, 625 (1933).

[19] P. J. Pagni and J. C. Keck, J. Chem. Phys. 58, 1162 (1973); R. M. Logan and J. C. Keck, *ibid.* 49, 860 (1968); P. J. Pagni, *ibid.* 58, 2940 (1973).

[20] J. E. Lennard-Jones and C. Strachan, Proc. R. Soc. (London) Ser. A 150, 442 (1935); J. E. Lennard-Jones and A. Devonshire, Proc. R. Soc. (London) Ser. A 156, 6, 29 (1936).

[21] B. Bendow and S. C. Ying, Phys. Rev. B 7, 622 (1973); 7, 637 (1973).

[22] B. J. Garrison, D. J. Diestler, and S. A. Adelman, J. Chem. Phys. 67, 4317 (1977); B. J. Garrison and S. A. Adelman, *ibid.* 67, 2379 (1977).

[23] T. N. Rhodin and D. L. Adams, in *Treatise on Solid State Chemistry*, edited by N. B. Hannay (Plenum, New York, 1976), Vol. 6AI.

[24] H. D. Hagstrum and E. G. McRae, Ref. 23.

[25] R. J. Madix, in *Physical Chemistry of Fast Reactions*, edited by D. O. Hayward (Plenum, New York, 1977).

[26] For recent reviews see (a) D. Menzel, in *Topics in Applied Physics*, edited by R. Gomer (Springer, Berlin, 1975), Vol. 4, p. 101; (b) T. E. Madey and J. T. Yates, Surf. Sci. 63, 203 (1977); (c) L. A. Peterman, in *Progress in Surface Science*, edited by S. G. Davison (Pergamon, New York, 1972), Vol. 3; (d) D. A. King, Surf. Sci. 47, 384 (1975); (e) D. Menzel, in *The Physical Basis for Heterogeneous Catalysis*, edited by E. Dragulis and R. I. Jaffee (Plenum, New York, 1975), p. 437.

[27] M. Born and K. Huang, *Dynamical Theory of Crystal Lattices* (Oxford University, London, 1954).

[28] H. C. Longuet-Higgins, Proc. Phys. Soc. (London) 60, 270 (1948).

[29] S. Epstein, J. Chem. Phys. 44, 836 (1966).

[30] S. Ichimaru, *Basic Principles of Plasma Physics* (Benjamin, Reading, Mass., 1973).

[31] A. L. Fetter and J. D. Walecka, *Quantum Theory of Many-Particle Systems* (McGraw-Hill, New York, 1971), pp. 390–399; V. Peuckert, Z. Phys. 241, 191 (1971); J. Harris and A. Griffin, Phys. Rev. B 11, 3669 (1975).

[32] L. I. Schiff, *Quantum Mechanics* (McGraw-Hill, New York, 1955).

[33] P. M. Morse, Phys. Rev. 34, 57 (1929).

[34] G. Herzberg, *Spectra of Diatomic Molecules* (Van Nostrand, New York, 1950).

[35] H. S. Heaps and G. Herzberg, Z. Phys. 133, 48 (1952).

[36] R. Herman and K. E. Shuler, J. Chem. Phys. 21, 373 (1953); 22, 954 (1954).

[37] L. Schmidt and R. Gomer, J. Chem. Phys. 42, 3573 (1965).

[38] G. Erlich, in *Advances in Catalysis* (Academic, New York, 1963), Vol. 14, p. 255.

[39] W. J. M. Rootsaert, L. L. van Reigen, and W. M. H. Sachtler, J. Catal. 1, 416 (1962).

[40] T. Engel and R. Gomer, J. Chem. Phys. 52, 5572 (1970).

[41] E. W. Montroll and K. E. Shuler, Adv. Chem. Phys. 1, 361 (1958).

[42] S. K. Kim, J. Chem. Phys. 28, 1057 (1958).

[43] J. L. Skinner and P. G. Wolyness, J. Chem. Phys. 69, 2143 (1978).

[44] D. R. Herschbach, in *Advances in Chemical Physics*, edited by J. Ross (Wiley, New York, 1966), Vol. 10.

[45] U. Fano, Phys. Rev. 124, 1866 (1961).

[46] O. K. Rice, Phys. Rev. 35, 1551 (1930).

[47] F. Mies and M. A. Krauss, J. Chem. Phys. 45, 4455 (1966); F. Mies, *ibid.* 51, 798 (1969).

[48] R. W. Numrich and K. G. Kay, J. Chem. Phys. 70, 4343 (1979), and references cited therein.

[49] M. Bixon and J. Jortner, J. Chem. Phys. 48, 715 (1968).

[50] M. Bixon and J. Jortner, J. Chem. Phys. 50, 4061 (1969); 48, 715 (1968).

[51] J. Jortner and S. Mukamel, in *The World of Quantum Chemistry*, edited by R. Daudel and B. Pullman (Reidel, Amsterdam, 1973).

[52] S. A. Rice, I. McLaughlin, and J. Jortner, J. Chem. Phys. 49, 5756 (1968).

[53] K. G. Kay and S. A. Rice, J. Chem. Phys. 57, 3041 (1972).

[54] E. J. Heller and S. A. Rice, J. Chem. Phys. 61, 936 (1974).

[55] D. F. Heller, M. L. Elert, and W. M. Gelbart, J. Chem. Phys. 69, 4061 (1978).

[56] S. Mukamel and J. Jortner, J. Chem. Phys. 65, 5204 (1976).

[57] R. J. Madix, *Surface Reaction-1979*, edited by U. Landman (AIP, New York, to be published).

[58] A doorway-state mechanism has been suggested in studies of multiphoton molecular fragmentation; for a recent review, see N. Blombergen and E. Yablonovitch, Phys. Today 31, 23 (1978).

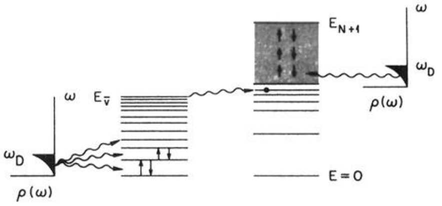

FIG. 8. Schematic picture of the door way-state model for thermal surface desorption or dissociation reaction mechanism. A characteristic Debye phonon density of states $\rho(\omega)$ is shown on the left and right. Excitation of a low-frequency, doorway, mode of vibration (typically a nonstretching mode) occurs via an incoherent multiphonon mechanism. Upon achieving the level $E_{\bar{v}}$ the excitation is transferred to the high-lying levels of a stretching mode (or comibnation of such modes) via anharmonic coupling. Further excitation in the dense vibrational manifold corresponding to the bond-rupture coordinate can occur via direct incoherent multiphonon excitations induced by thermal coupling to the substrate. The predissociation level is denoted by E_{N+1}. Having achieved this level the reaction proceeds through coupling to possible final-state channels such as dissociation, desorption, or migration.